*Korean J. of Chem. Eng.*, 9(4), 186-193 (1992)

# ANALYSIS ON THE APPARENT SLIP AND DEPLETED LAYER OF POLYMER FLOW IN NARROW-BORE CAPILLARIES

**Cheon-Il Park*, Myung-Suk Chun, Dong-Hak Kim and O Ok Park****

Department of Chemical Engineering, Korea Advanced Institute of Science and Technology, 373-1, Kusong-Dong, Yusung-Ku, Taejon 305-701, Korea

*(Received 22 May 1992 • accepted 28 September 1992)*

**Abstract**—Polymer solutions flowing through small-diameter capillaries of which length scale is much larger than that of polymers were experimentally demonstrated to have the enhanced flow rate as compared to in bulk flow. This *apparent slip phenomenon* was analyzed by obtaining the *slip velocity* and concentration *depleted layer thickness*. Hydrolyzed polyacrylamide (HPAM) of highly flexible polymer and Xanthan of rigid rodlike polymer were made to flow through stainless steel capillaries having the diameter range of about 100 to 250 μm. The results showed that both slip velocity and depleted layer thickness decreased markedly with increasing polymer concentration. This behavior can be interpreted as being due to the reduction of diffusion coefficient and flexibility of polymer chains as the concentration is increased. The depleted layer thickness of HPAM was much larger than the polymeric length scale and was shown to increase with increasing wall shear stress. This is considered as an evidence of the *stress-induced diffusion* of polymer chains being a dominant factor for the apparent slip of flexible polymer solution. On the other hand, the depleted layer thickness of Xanthan solution was almost constant with the wall shear stress, which can not be explained by the stress-induced diffusion mechanism alone.

## INTRODUCTION

The flow of polymer solutions through porous media has been the subject of experimental and theoretical investigations. Such studies are relevant to a number of phenomena, including applications of polyelectrolytes in enhanced oil recovery, chromatography, and filtration process. Since in most of these applications the polymer solution is confined to narrow regions of space, it is important to investigate the behavior of the polymer near a wall and in the presence of a flow field.

It is obvious that flow of polymers in a confined geometry is different from those in the infinite domain. It may be helpful to classify two distinct cases based on the relative size of polymer to that of confining geometry. If they are comparable with each other, it is easy to formulate theoretical problem with the help of molecular models such as elastic dumbbell for flexible chains and rigid dumbbell model for rigid chains [1, 2]. However, its experimental verification is somewhat complicated due to the difficulty of obtaining well defined flows in such a small scale. In this context, Chauveteau [3] performed excellent experiments on flows of Xanthan solutions through the well-defined cylindrical micropores to obtain that the shear viscosity decreases as size of pore decreases because of the concentration depleted layer formed near a wall of pore.

On the other hand, if the relative size of confining geometry is much larger than that of polymers, then the situation is totally different. Viscosity reduction was observed on a rather large scale to be explained with the depleted layer of molecular scale. Cohen [4] and Cohen and Metzner [5] achieved such flowing experiments of several polymer solutions through a narrow capillary to see apparent viscosities decrease as the diameter of the capillary decreases. They interpreted it as an apparent slip and developed a systematic analytical scheme to calculate not only the thickness of a slip layer but also a slip velocity.

*current address: PE Product Department, HanYang Chemical Corp., Daeduk Research Center, Shinsung-Dong, Yusung-Ku, Taejon

**To whom any correspondence should be addressed.

In order to explain such a slip phenomenon, the stress-induced diffusion mechanism was introduced by Tirrell and Malone [6] and Metzner et al. [7]. If the length scale of confining geometry is large enough to generate an inhomogeneous flow field, then the polymer in higher shear stress region will tend to migrate to lower stress region, or inward to the center of tube. Therefore, there may be a polymer concentration depleted layer near the wall of which thickness is much thicker than the polymer characteristic length. Here we are going to restrict ourselves to the latter case to demonstrate that not only a relative molecular scale to the size of confining geometry but also a wall shear stress will play the major roles to determine the apparent slip and depleted layer. Furthermore, it will be shown that the flexible polymer exhibits slightly different behaviors compared with those of rigid one flowing in the confined geometry.

## EXPERIMENTAL

### 1. Polymers

Polymers used for this work are Xanthan biopolymer and partially hydrolyzed polyacrylamide (HPAM), which represent rigid and flexible polymer chains, respectively. Xanthan was purchased from Sigma Co. as a practical grade and its weight-average molecular weight $M_w$ is about $3.8\times10^6$. Polyacrylamide was obtained from Aldrich Co. as powder, of which $M_w$ is $2.0\times10^5$. Distilled water was used as solvent for both polymers.

For a rigid rodlike polymer like Xanthan, it was suggested to evaluate macromolecular dimensions from the intrinsic viscosity data (see, e.g., Ref. 3). If length-to-diameter ratio p is large enough (p>50), then viscosity factor $v_o=[\eta]_o/v_{sp}$ can be approximated by the power law function:

$$v_o=0.159\,p^{1.801}. \tag{1}$$

Here, $v_{sp}$ is the specific volume, equal to 0.62 for oligosaccharides. The value of p was calculated as 425 according to the experimental intrinsic viscosity of Xanthan, 5340 $cm^3/g$. Once the value of p is given, the equivalent characteristic length of Xanthan, $L_r$ can be estimated from

$$L_r^3=\frac{45}{2\pi N_A}[\eta]M_w\ (\ln 2p-0.5) \tag{2}$$

where $N_A$ is Avogadro's number. $L_r$ was calculated as 1.154 μm, which is nearly consistent with the result reported elsewhere by Chun et al. [8].

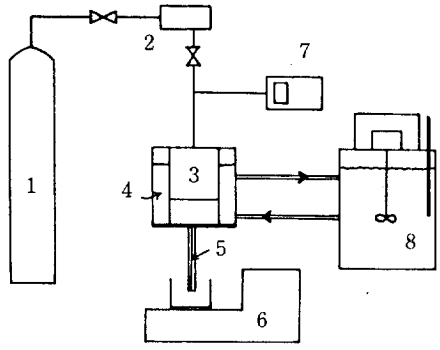


**Fig. 1. Schematic diagram of experimental apparatus.**

1. $N_2$ gas tank
2. Pressure regulating system
3. Solution reservoir
4. Water-jacket
5. Stainless steel capillary
6. Electronic analytical balance
7. Digital manometer
8. Constant temperature bath

For a flexible polymer chain like HPAM, Wang [9] correlated the relationship between intrinsic viscosity and characteristic length of polymers from gel permeation chromatography:

$$[\eta]=1.67\times10^{-8}\ \langle L_f^2\rangle^{2.97/2}. \tag{3}$$

Here $\langle L_f^2\rangle^{1/2}$ and $[\eta]$ have units of Å and dl/g. With the experimental correlation between intrinsic viscosity $[\eta]$ and known molecular weight $M_w$ (see, e.g., Refs. 4 and 10):

$$[\eta]=3.13\times10^{-3}\,M_w^{0.77}. \tag{4}$$

The equivalent characteristic length of HPAM, $L_f$ was obtained as 0.14 μm.

In the case of Xanthan, 500 ppm (=0.05%) was chosen for the concentration. And for HPAM, the concentrations of 1000, 2000, 3000, and 5000 ppm were considered. Polymers were dissolved by using the magnetic stirrer with a condition of minimum speed in order to reduce any possibility of the degradation of polymer chains. After that they were filtered through cellulose ester membranes (Gelman Science) with a low flow rate to get rid of any solid particles, suspensions or microgel.

### 2. Experimental Set-up

Narrow-bored capillary rheometer was made to measure the rheological properties of polymer solution, which is mainly composed of three parts. Solution reservoir, inert nitrogen gas tank to generate the pressure drop for flow, and flow rate measuring system are shown in Fig. 1. Solution reservoir will supply the

**Table 1. Dimensions of the capillaries (unit in μm)**

| Capillary | Nominal diameter | Diameter measured (=D) | $L_e/D$ |
|---|---|---|---|
| A | 254.0 | 237.8 | 663 |
| B | 177.8 | 199.5 | 629 |
| C | 101.6 | 100.9 | 679 |

solutions to different size of capillaries with the pressure of gas tank. It was manufactured from acryl resin, which is a cylindrical vessel of 12.0 cm in length and 7.5 cm in diameter with water-jacketed. Temperature was controlled to be maintained at 25℃. Pressure was generated by nitrogen gas tank with pressure regulating system and was measured with digital manometer, of which the accuracy is order of $\pm(1\times10^{-3})$ atm. Flow rate from the narrow-bore capillary was measured using an electronic analytical balance (Mettler, AE 200) with $\pm10^{-4}$g accuracy. After the minimum 3 minutes at each measurements, flow rate was chosen for accuracy. Narrow-bore capillaries used were purchased from Alltech Inc. (Illinois, USA). They are made of 1/16" OD stainless steel tube of which dimensions are tabulated in Table 1. Diameter was estimated with the distilled water having known viscosity by using Hagen-Poiseuille equation (see, Ref. 11):

$$Q=\Delta p\frac{\pi D^4}{128\,\mu L_e} \tag{5}$$

where $L_e$ is the narrow-bore capillary length.

To be sure that there is no polymer adsorbed on the wall of the capillary, the procedure suggested by Cohen and Metzner [12] was adopted. In order to eliminate adsorption effects, they treated the inner surface of capillaries by using a coating procedure with the silane compound, such as a solution of 2% dimethyldichlorosilane in an ethanol-water solution. Temperature control was provided by circulating water from a constant temperature bath around the reservoir through a water-jacket. Both the reservior and the capillary were thoroughly insulated.

## 3. Data Analysis

The slip velocity at a wall can be estimated from apparent shear rate $\dot\gamma_a$ and shear stress $\tau$ data with three different capillaries. Flow rate of laminar tube flow is obtained from the velocity distribution as following:

$$Q=\int_0^R u(r)2\pi r\,dr$$
$$=\pi\int_0^{R^2} u\,d(r^2) \tag{6}$$

where R is the capillary tube radius, and u is the fluid velocity. It can be converted into the following expression by using integration by parts scheme.

$$Q=\pi u_s R^2-\pi\int_0^R r^2(du/dr)\,dr \tag{7}$$

where $u_s$ is the slip velocity. The shear rate can be related as a function of shear stress $f(\tau)$ and the shear stress is linear in radial position r, or $\tau/\tau_w=r/R$. Then, we have

$$Q=\pi u_s R^2+\frac{\pi R^3}{\tau_w^3}\int_0^{\tau_w}\tau^2 f(\tau)\,d\tau. \tag{8}$$

Here $\tau_w$ is the wall shear stress, which is proportional to the pressure drop:

$$\tau_w=\Delta p/(4L_e/D). \tag{9}$$

Eq. (8) can be converted into a relationship between apparent shear rate $\dot\gamma_a$ and wall shear stress:

$$\dot\gamma_a=\frac{32Q}{\pi D^3}$$
$$=\frac{4}{\tau_w^3}\int_0^{\tau_w}\tau^2 f(\tau)\,d\tau+\frac{8u_s}{D}. \tag{10}$$

Therefore, in order to evaluate the slip velocity, apparent shear rate should be differentiated with respect to (1/D):

$$u_s=\frac{1}{8}\left(\frac{\partial(32Q/\pi D^3)}{\partial(1/D)}\right)\Big|_{\tau_w}. \tag{11}$$

In order to calculate the depleted layer thickness $\delta$, let us suppose a depleted layer of polymer concentration near the wall, of which rheological properties are defined by $\dot\gamma=-g(\tau, c)$ instead of $\dot\gamma=-f(\tau, c_o)$ of bulk flow. Here c is the polymer concentration in the depleted layer, and $c_o$ is the bulk concentration of polymers. Then flow rate can be expressed as a sum of two terms:

$$\frac{32Q}{\pi D^3}=\frac{4}{\tau_w^3}\int_0^{\tau_\delta}\tau^2 f(\tau, c_o)\,d\tau+\frac{4}{\tau_w^3}\int_{\tau_\delta}^{\tau_w}\tau^2 g(\tau, c)\,d\tau \tag{12}$$

where $\tau_\delta$ is shear stress at the depleted layer position of R-$\delta$. If we combine this equation with Eq. (10), then slip velocity $u_s$ is expressed by:

$$u_s=\frac{R}{\tau_w^3}\left[\int_{\tau_\delta}^{\tau_w}\tau^2 g(\tau, c)\,d\tau-\int_{\tau_\delta}^{\tau_w}\tau^2 f(\tau, c_o)\,d\tau\right]. \tag{13}$$

Since the depleted layer thickness is much smaller than the radius of capillary, $f(\tau, c_o)$ is assumed to be equal to that of bulk flow. If power law model is as-

sumed, then $\tau = K \cdot f(\tau, c_o)^n$. On the other hand, the $g(\tau, c)$ for depleted layer can be assumed to be linear in shear stress as first approximation:

$$g(\tau, c) = g(\tau_w, c_w) - [g(\tau_w, c_w) - f(\tau_\delta, c_o)] (\tau_w - \tau)/(\tau_w - \tau_\delta) \quad (14)$$

where, $c_w$ is the polymer concentration at wall. Now Eq. (14) is substituted into Eq. (13) and if terms up to $O(\delta/R)$ are retained, then

$$u_s = (1/2)\ \delta[g(\tau_w, c_w) - f(\tau_\delta, c_o)]. \quad (15)$$

Here we know that $\tau_\delta = \tau_w(1-\delta/R)$, and $g(\tau_w, c_w)$ is much larger than $f(\tau_\delta, c_o)$ so that $f(\tau_\delta, c_o)$ can be neglected. Indeed, we have

$$u_s = (1/2)\ \delta\ g(\tau_w, c_w). \quad (16)$$

Therefore, if $u_s$ and $g(\tau_w)$ are determined experimentally, then the depleted layer thickness can be estimated at that shear stress $\tau_w$.

$g(\tau_w)$ can be calculated from the following Eq. (17) which is obtained by differentiating both sides of Eq. (12) by $\tau_w$:

$$g(\tau_w) = \dot{\gamma}_w = (3 + 1/m)(Q/\pi R^3). \quad (17)$$

Here $\dot{\gamma}_w$ is wall shear rate, and m is obtained from the log-log plot of apparent shear rate and shear stress. As it is seen, Eq. (17) is the same as Rabinowitsch equation, which leads to the fact that Rabinowitsch equation can be used irrespective of the existence of concentration depleted layer.

## RESULTS AND DISCUSSION

### 1. End Effect

Generally the measured pressure drop $\Delta p_m$ is determined between the capillary exit and somewhere above the entry. This measured pressure drop includes excess pressure drops $\Delta p_e$ due to entry and exit effects [4]. In order to evaluate the rheological properties from tube flow data, excess pressure drop should be excluded first. Bagley [13] method can be used for this purpose. Then we have

$$\Delta p_m = 4\tau_w(L_e/D + L_c/D) \quad (18)$$

where $\Delta p_e$ can be obtained from shear rate-shear stress plots with several different lengths $L_c$. For capillary A, experimental data for shear rate-shear stress of three different lengths (i.e., 6.35, 5.3 and 4 cm) fall into a single curve as shown in Fig. 2 so that the end effect can be neglected in this work.

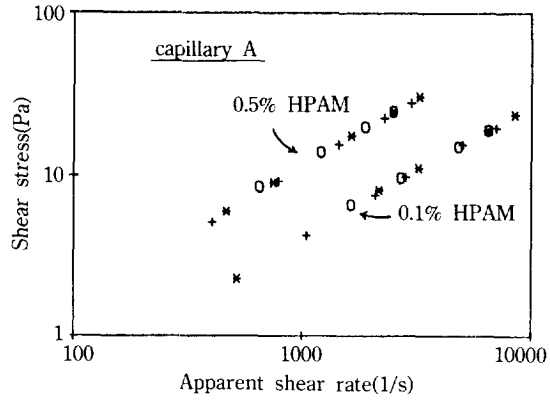


**Fig. 2. Flow curves of 0.1 and 0.5% HPAM solutions for various capillary lengths: $L_c$ = 6.35 cm (○), 5.3 cm (*), 4.0 cm (+), capillary A was used.**

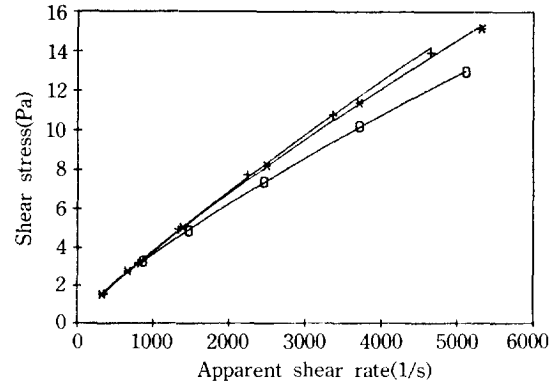


**Fig. 3. The flow curve of 0.1% HPAM solution for three different capillaries: capillary A (+), B (*), and C (○), (see, Table 1 for dimensions).**

### 2. Flow and Viscosity Curves

Typical flow curve for 0.1% HPAM is shown in Fig. 3 as plots of apparent shear rate vs shear stress for three different capillary diameters. As the diameter of the capillary is reduced, apparent slip, or flow enhancement is increased. 0.2 and 0.3% HPAM solutions show the similar tendency, while 0.5% HPAM solution shows no a difference in flow curves between capillary A and B. Fig. 4 shows the case of 0.05% Xanthan solution. From these curves, if we use Eq. (17) for shear rate, then viscosity curves can be obtained as shown in Figs. 5 and 6. Here one can easily observe a main difference between two plots. HPAM solution shows a decreasing tendency in power law index n as the diameter of capillary decreases, but no difference is detected for Xanthan solution.

For flexible chain like HPAM, as the diameter of

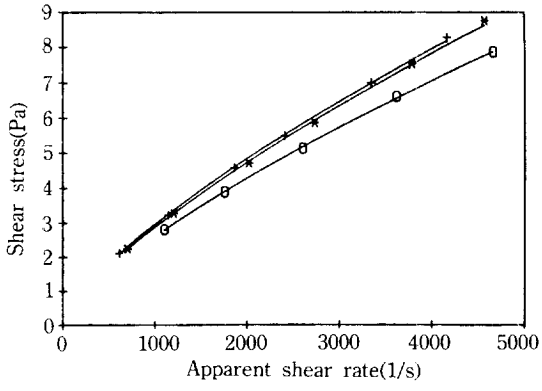


**Fig. 4. The flow curve of 0.05% Xanthan solution for three different capillaries: capillary A (+), B (*), and C (○).**

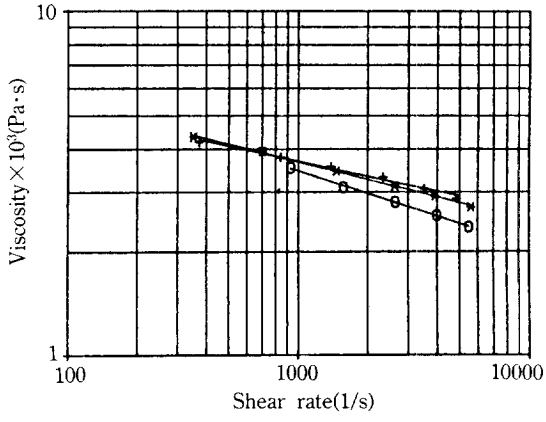


**Fig. 5. The viscosity curve of 0.1% HPAM solution for three different capillaries: capillary A (+), B (*), and C (○).**

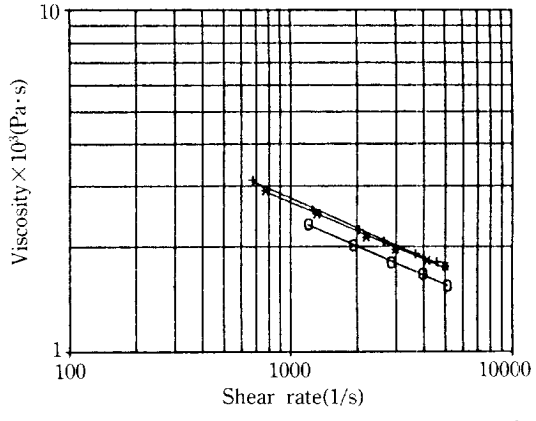


**Fig. 6. The viscosity curve of 0.05% Xanthan solution for three different capillaries: capillary A (+), B (*), and C (○).**

**Table 2. Parameters of power law model**

| Polymer solution | Capillary diameter(μm) | n | K (Pa·sec$^n$) |
|---|---|---|---|
| 0.1% | 237.8 | 0.8539 | 0.01011 |
| (=1000 ppm) | 199.5 | 0.8291 | 0.01195 |
| HPAM | 100.9 | 0.7787 | 0.01596 |
| 0.2% | 237.8 | 0.8242 | 0.01976 |
| (=2000 ppm) | 199.5 | 0.8273 | 0.01867 |
| HPAM | 100.9 | 0.7540 | 0.02948 |
| 0.3% | 237.8 | 0.8030 | 0.03025 |
| (=3000 ppm) | 199.5 | 0.8177 | 0.02646 |
| HPAM | 100.9 | 0.7247 | 0.04997 |
| 0.05% | 237.8 | 0.7134 | 0.02001 |
| (=500 ppm) | 199.5 | 0.7255 | 0.01787 |
| Xanthan | 100.9 | 0.7193 | 0.01693 |

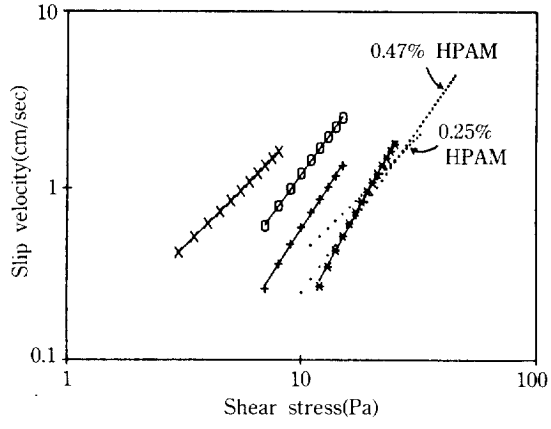


**Fig. 7. Slip velocity as a function of wall shear stress for HPAM and Xanthan solution: 0.1% HPAM (○), 0.2% HPAM (+), 0.3% HPAM (*), 0.05% Xanthan (×), and dotted lines from Ref. 13.**

capillary decreases, the concentration depleted layer will increase relatively by stress-induced diffusion, which results in a reduction of viscosity. On the other hand, for rigid chain like Xanthan, there could be a balance between stress-induced diffusion and concentration redistribution. This feature seems to be due to the parallel orientation of Xanthan since rigid rod-like chain cannot be deformed much by applied stress, but its orientation can be aligned along the wall [8]. The depleted layer thickness calculated later will support this argument, since the order of depleted layer is three times of its macromolecular scale. Parameters of power law model are tabulated in Table 2. These data can be analyzed *via* depleted layer thickness and slip velocity.

## 3. Slip Velocity and Depleted Layer Thickness

**Table 3. Parameters in slip velocity**

| Polymer solution | a [m/(sec·Pa$^b$)] | b | $\tau_w$ (Pa) |
|---|---|---|---|
| 0.1% HPAM | $2.88\times10^{-8}$ | 1.873 | 7-15 |
| 0.2% HPAM | $1.94\times10^{-9}$ | 2.158 | 7-15 |
| 0.3% HPAM | $4.27\times10^{-11}$ | 2.543 | 12-25 |
| 0.05% Xanthan | $1.62\times10^{-6}$ | 1.378 | 3-8 |

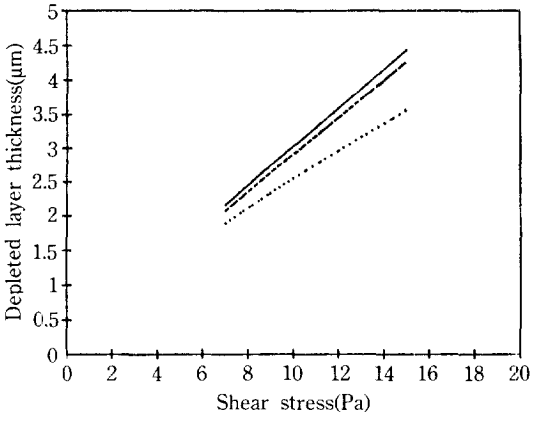


**Fig. 8. Depleted layer thickness as a function of wall shear stress for 0.2% HPAM: capillary A (—), B (---), C (···).**

According to Eq. (11) the slip velocity can be obtained from the plot of 1/D vs apparent shear rate. Slip velocity can be correlated with wall shear stress as shown in Fig. 7. Slip velocity does not depend upon the diameter of the capillary which is consistent with the results reported by Cohen and Metzner [5]. If one use a linear correlation between slip velocity and wall shear stress, then

$$u_s = a\tau_w^b \tag{19}$$

where, a and b are tabulated in Table 3. The reason why slip velocity decreases as polymer concentration increases is that the diffusivity and flexibility of polymer chains will be decreased as the concentration increases. For a comparison, data obtained by Cohen [4] are plotted together. The overall magnitude is consistent, however, the slope is much different due to the flexibility of HPAM chains depending upon the hydrolyzed extent.

For the better parameter which explains the slip phenomenon, depleted layer thickness can be estimated by Eq. (16). Fig. 8 shows that depleted layer thickness increases as wall shear stress increases for HPAM solutions, which is consistent with the results from stress-induced diffusion. As wall shear stress increases the polymer chains experienced with high shear will propagate inward the capillary tube due to the entropic force to result in 1.5-5 μm which are of about 15-35 times larger than that of macromolecular scale (i.e., 0.14 μm). Now, it is obvious that the repulsive wall effect is not the only reason of such slip phenomena but stress-induced diffusion effect is a lot more than that. It can be easily understood when one replots δ/R vs shear stress as Fig. 9. The relative location of depleted layer is almost constant regardless of concentration and flexibility of polymer. However, δ/R values of capillary C are somewhat larger than those of capillary A and B. This may be due to the fact that the concentration profile in a capillary develop more rapidly as capillary diameter decreases, which

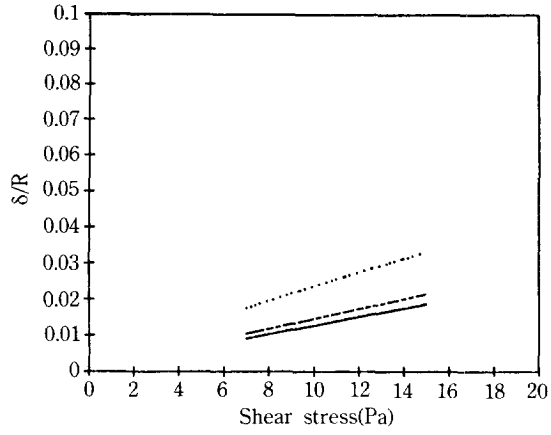


**Fig. 9. Reduced depleted layer thickness δ/R as a function of wall shear stress for 0.2% HPAM solution: capillary A (—), B (---), C (···).**

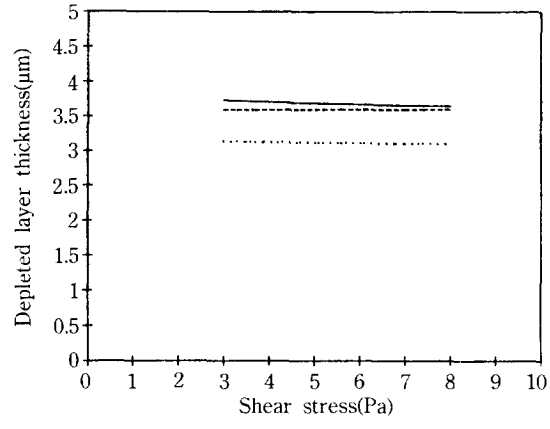


**Fig. 10. Depleted layer thickness as a function of wall shear stress for 0.05% Xanthan solution: capillary A (—), B (---), C (···).**

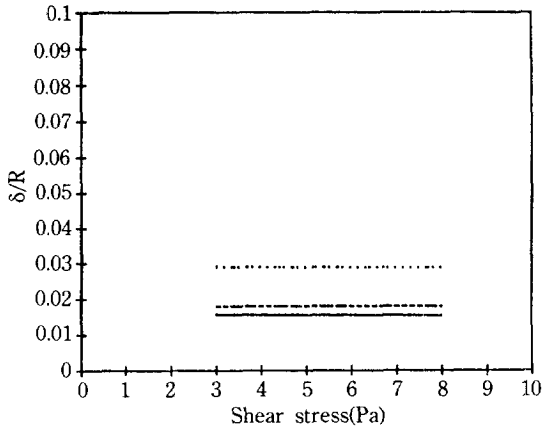


**Fig. 11. Reduced depleted layer thickness δ/R as a function of wall shear stress for 0.05% Xanthan solution: capillary A (—), B (---), C (···).**

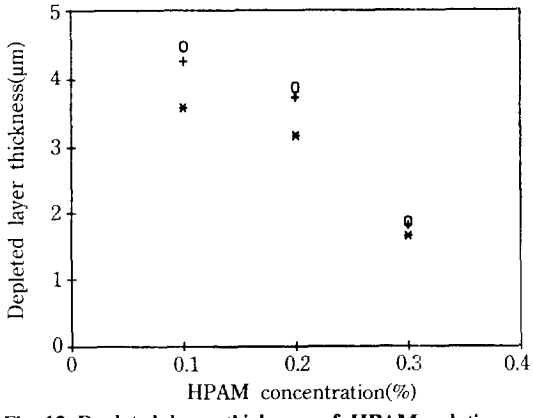


**Fig. 12. Depleted layer thickness of HPAM solution as a function of polymer concentration at $\tau_w = 13$ Pa: capillary A (○), B (+), and C (*).**

is proposed by Tirrell and Malone [6]. Situation for rigid rodlike polymer is slightly different. As shown in Fig. 10, depleted layer thickness is not dependent upon wall shear stress, and only about three times larger than that of macromolecules as shown in Fig. 11. But the relative location of depleted layer is as same as that of flexible one.

Recently, Omari et al. [14] observed that the depleted layer thickness decreases as wall shear rate increases for Xanthan solution flowing through microporous membranes, which can be compared with our constant depleted layer. In their case, micropores are not long enough to have a fully developed flow so that with increasing shear, polymers can be aligned parallel to the wall which results in the decrease of depleted layer. In our case, however, the flow is fully developed so that even parallelly aligned polymer can migrate inward to the tube center due to the stress-induced diffusion, which may be balanced with outward migration due to the parallel alignment. Fig. 12 shows the depleted layer thickness decreases with increasing polymer concentration as the slip velocity does. The possible explanation is the same as before.

## CONCLUSIONS

Polymer molecules may be excluded from a region of fluid close to the wall in a narrow capillary, this effect results in a concentration depleted layer which causes both apparent slip and velocity enhancement of polymers relative to the solvent. We find that the slip and depleted layer phenomena for flexible polymers such as a HPAM solution are strongly affected by the stress-induced diffusion. Experimental results clearly indicate these phenomena, which results give almost constant relative location of depleted layer in the capillary and show the increasing depleted layer according to shear stress. In the case of somewhat rigid chain like Xanthan, the depleted layer thickness is almost constant regardless of stress as a result of balancing the parallel orientation and stress-induced diffusion.

## ACKNOWLEDGEMENT

This work was supported by Fundamental Research Grant (911-1001-004-2) from the Korea Science and Engineering Foundation. Authors gratefully acknowledge financial support from the KOSEF.

## NOMENCLATURE

| | |
|---|---|
| a, b | : parameters in slip velocity |
| c | : polymer concentration in depleted layer |
| $c_0$ | : bulk concentration of polymers |
| $c_w$ | : polymer concentration at wall |
| D | : capillary diameter |
| K | : power law constant |
| $L_c$ | : capillary length |
| $L_e$ | : equivalent capillary length |
| $L_f$ | : equivalent characteristic length of HPAM |
| $L_r$ | : equivalent characteristic length of Xanthan |
| $M_w$ | : weight-average molecular weight |
| m | : slope at log-log plot of apparent shear rate vs shear stress |
| $N_A$ | : Avogadro's number |
| n | : power law index |

p : length-to-diameter ratio
$\Delta p$ : pressure drop of capillary
$\Delta p_e$ : excess pressure drop
$\Delta p_m$ : measured pressure drop
Q : volumetric flow rate
R : capillary radius
r : radial position
u : fluid velocity
$u_s$ : slip velocity
$v_n$ : viscosity factor
$v_{sp}$ : specific volume

**Greek Letters**

$\dot{\gamma}$ : shear rate
$\dot{\gamma}_a$ : apparent shear rate
$\dot{\gamma}_w$ : wall shear rate
$\delta$ : depleted layer thickness
$[\eta]$ : intrinsic viscosity
$[\eta]_o$ : Newtonian intrinsic viscosity
$\mu$ : Newtonian fluid viscosity
$\tau$ : shear stress
$\tau_w$ : wall shear stress
$\tau_\delta$ : shear stress at the depleted layer position of R-$\delta$

## REFERENCES


1. Aubert, J. H. and Tirrell, M.: *J. Chem. Phys.*, **77**, 553 (1982).
2. Brunn, P. O.: *J. Rheol.*, **29**, 859 (1985).
3. Chauveteau, G.: *J. Rheol.*, **26**, 111 (1982).
4. Cohen, Y.: Ph. D. Dissertation, Univ. of Delaware, Newark (1981).
5. Cohen, Y. and Metzner, A. B.: *J. Rheol.*, **29**, 67 (1985).
6. Tirrell, M. and Malone, M. F.: *J. Polym. Sci., Polym. Phys. (Ed.)*, **15**, 1569 (1977).
7. Metzner, A. B., Cohen, Y. and Rangel-Nafaile, C.: *J. Non-Newtonian Fluid Mech.*, **5**, 449 (1979).
8. Chun, M.-S., Park, O. O. and Kim, J. K.: *Korean J. of Chem. Eng.*, 7(2), 126 (1990).
9. Wang, F. H. L.: Ph. D. Thesis, Penn. State Univ. (1978).
10. Flory, P. J.: "Principles of Polymer Chemistry", Cornell Univ. Press (1953).
11. Bird, R. B., Stewart, W. E. and Lightfoot, E. N.: "Transport Phenomena", John Wiley & Sons Inc. (1960).
12. Cohen, Y. and Metzner, A. B.: *Macromolecules*, **15**, 1425 (1982).
13. Bagley, E. B.: *J. Appl. Phys.*, **28**, 624 (1957).
14. Omari, A., Moan, M. and Chauveteau, G.: *J. Rheol.*, **33**, 1 (1989).